

# Influence of Aspect Ratio on the Performance of Outboard-Horizontal-Stabilizer Aircraft

J. A. C. Kentfield\*

University of Calgary, Calgary, Alberta, Canada T2N 1N4

A brief description is given of the outboard-horizontal-stabilizer concept and relevant background material. Wind-tunnel tests were conducted to investigate the influence of main-plane aspect ratio on the flowfields prevailing in the vicinity of the tail surfaces located essentially downwind of the wing tips. It was found that variation of aspect ratio had, for a prescribed wing lift coefficient, substantially zero influence on the flow pattern. Partly as a consequence of this finding, simple equations were derived describing the flowfields interacting with the tail surfaces. These analytical results were employed in predicting the performance of optimized outboard horizontal stabilizer aircraft covering a range of aspect ratios from 6 to 15. It was concluded that these aircraft had cruise drag values between 20 and 45% less, with planform areas typically 15% lower, than those of comparable conventional aircraft.

## Nomenclature

$A$	= aspect ratio
$a$	= downwind displacement of c.g. from $(c_w/4)$
$C_{DO}$	= two-dimensional drag coefficient (of airfoil)
$C_L$	= lift of coefficient
$C_M$	= pitching moment coefficient (nose up positive)
$c$	= average chord
$D$	= drag of aerodynamic surfaces
$e$	= Oswald efficiency factor
$L$	= lift of aerodynamics surfaces
$L'$	= distance from $c_w/4$ to $c_{TH}/4$
$n$	= multiple of $c_w$ (origin at outboard face of tail boom)
$S$	= planform area
$U$	= flight velocity
$w$	= downwash velocity (positive downward)
$Y$	= (displacement from midspan)/(semispan)
$\varepsilon$	= downwash angle (positive downward)
$\theta$	= pitch static margin [ $\equiv$ (distance from c.g. to neutral point)/ $c_w$ ]

## Subscripts

$c/4$	= quarter-chord location
$L$	= lateral inflow (operates on $\varepsilon$ to change sign to positive toward aircraft centerline)
$TH$	= tail (horizontal)
$TV$	= tail (vertical)
$U$	= upwash (operates on $\varepsilon$ to change sign to positive upward)
$W$	= wing

## Introduction

THE outboard-horizontal-stabilizer (OHS) concept is one in which tail surfaces are supported on downwind-projecting booms attached to each tip of a monoplane wing. Specifically, each horizontal tail surface projects outboard, only, of the boom to which it is attached such that it is immersed in the upwash flow formed outboard, and downwind, of the wing tip. This configuration permits the horizontal tail surfaces to provide not only pitch control, as in a conventional aircraft, but also to serve as efficient lift generators due to the tail lift vectors being inclined forward, due to the upwash flow, hence generating a thrust component that helps to offset drag.

Received 1 November 1998; revision received 17 June 1999; accepted for publication 27 July 1999. Copyright © 1999 by J. A. C. Kentfield. Published by the American Institute of Aeronautics and Astronautics, Inc., with permission.

\*Professor, Department of Mechanical and Manufacturing Engineering, Senior Member AIAA.

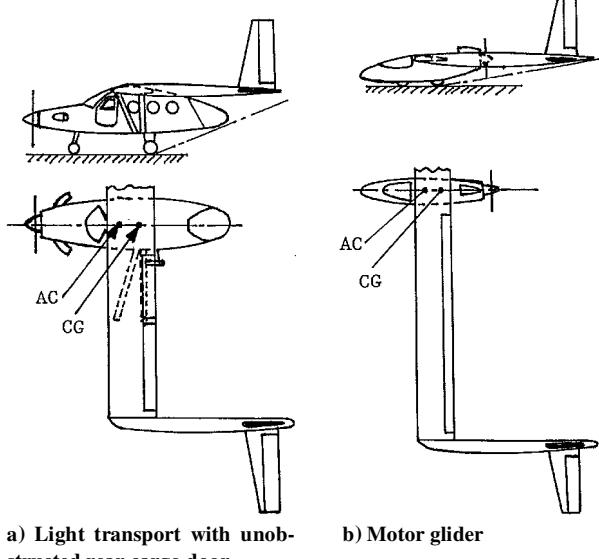
The c.g. of an OHS design is generally farther aft than that of a conventional configuration to counterbalance the tail lift. The tail lift coefficient is arranged to be approximately half that of the wing to provide a substantial margin for pitch control.

Because the lift generated by the horizontal tail surfaces is additional to that produced by the aircraft main-plane, the wing area of an OHS aircraft will be smaller than that of a conventional aircraft of equal gross lift for which the tail does not generate any lift or, more commonly, a small, negative lift. Furthermore, flows over OHS vertical tail surfaces, also attached to the downwind ends of the booms, benefit from an inward inclination toward the aircraft longitudinal centerline. This situation gives rise to the generation, in a horizontal plane, of aerodynamic lift. The vectors representing this lift are tilted forward and hence contribute to producing a thrust that also tends to counter drag much in the manner of conventional winglets.

The prime objective of the present study was to establish the influence of main-plane aspect ratio on the performances of OHS aircraft configurations relative to those of corresponding conventional designs of equal aspect ratio. An additional objective was to perform such a comparison using designs that were, at least to a first order of approximation, optimized from an aerodynamic perspective. Recent prior work was based on a more conservative approach and on a single OHS main-plane aspect ratio  $A_w$  of six (Ref. 1). Figure 1a illustrates a possible configuration of a light transport aircraft that not only benefits from the advantages of the OHS concept identified earlier but also offers the additional advantage of an unobstructed rear cargo door suitable for vehicle access. Figure 1b shows an OHS-type motor glider, or similar aircraft, featuring a high aspect ratio wing, that would, in all probability, employ laminar-flow-type aerodynamic surfaces.

## Background

Early work at the University of Calgary on the OHS concept included wind- and water-tunnel tests allowing comparisons to be made between OHS and comparable conventional configurations.<sup>2,3</sup> The prior work also included aerodynamic performance predictions and a preliminary load analysis.<sup>1,3–6</sup> The indications of this work were that OHS aircraft offered the potential for significant drag reductions relative to conventional designs and also that the OHS concept is feasible from a structural viewpoint. In addition, it has been demonstrated, by University of Calgary students, that OHS aircraft are capable of controlled flight. The students have built and flown, successfully, large-scale, radio-controlled, powered, model OHS-type aircraft of approximately 3-m ( $\approx 10$ -ft) span. Very recently, an 18% of full-scale OHS model has been constructed and test flown by Scaled Composites, Inc. This model is representative of a high-altitude, environmental monitoring, uninhabited air vehicle



a) Light transport with unobstructed rear cargo door      b) Motor glider

Fig. 1 OHS type aircraft.

(UAV) with a full-scale span of 31.4 m (103 ft) designed by Scaled Composites for NASA.

Work undertaken prior to that at the University of Calgary and also at Scaled Composites involves, to the best of the writer's knowledge, three full-scale aircraft and model gliders. Toward the end of the Second World War, the Chance Vought Company produced an ultralow aspect ratio light research aircraft, the V173. This vehicle was equipped with horizontal stabilizers projecting outboard of the wing tips with trailing edges of the stabilizers aligned with the wing trailing edge.<sup>7</sup> Later, a much heavier prototype fighter, powered by two piston engines, identified as the XF5U-1 was produced by Chance Vought but was never test flown.<sup>7,8</sup> An even earlier development took place in Germany at the Blohm und Voss Company. This aircraft was a single-engined, pusher-type, piston-engined fighter with aft-swept wings. Pitch control was by means of two horizontal stabilizer surfaces, each mounted on a very short boom with the leading edge of each stabilizer aligned with the wing trailing edge.<sup>9</sup> More recently, work was undertaken using model gliders with configurations similar to those of Fig. 1, but with horizontal stabilizer surfaces that projected somewhat inboard as well as outboard of downwind-projecting, wing-tip-mounted, support booms (private communication with C. W. McCutchen, Washington, DC, 16 October 1991).

## Test Results

### Tip-Vortex Correlation

Because the main objective of the present study was to establish the influence of the main-plane aspect ratio on the performance of OHS-type aircraft, it became necessary to obtain an understanding of the vortex flows prevailing downwind of, but fairly close to, wing tips as a function of both wing lift coefficient  $C_{LW}$  and wing aspect ratio  $A_W$ . Prior information of this type available to the writer related, specifically, to an aspect ratio of six only.<sup>1</sup> It was proposed to establish the required data experimentally by wind-tunnel tests conducted on a wing of invariant cross-sectional dimensions but of variable aspect ratio. However, a potential problem relating to this approach was that the facilities available restricted the tests to turbulent flow with a wing-chord-based Reynolds number of only  $6 \times 10^4$ .

Although the separated, vortexlike flow in the region of a wing tip was not expected to be a strong function of Reynolds number, it was thought desirable to verify this assumption by comparing results obtained in the writer's facility with data obtained at significantly higher Reynolds numbers. Such a comparison is presented in Fig. 2 which shows plots of upwash flow angles  $\epsilon_U$  vs the displacement outboard of a tail-support boom of thickness 0.1  $c_W$ , measured as multiples  $n$  of the chord of the rectangular planform

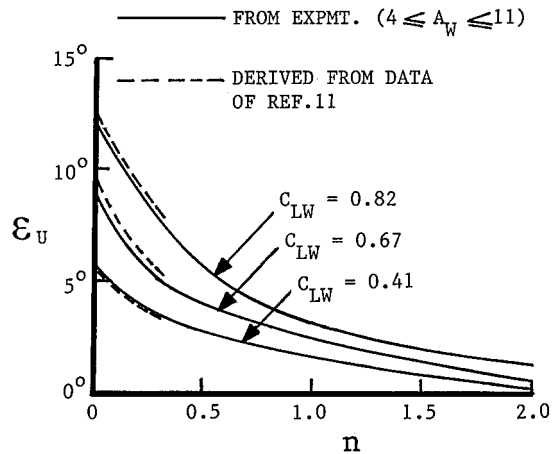


Fig. 2 Comparison of upwash flow measurements (no tail surfaces).

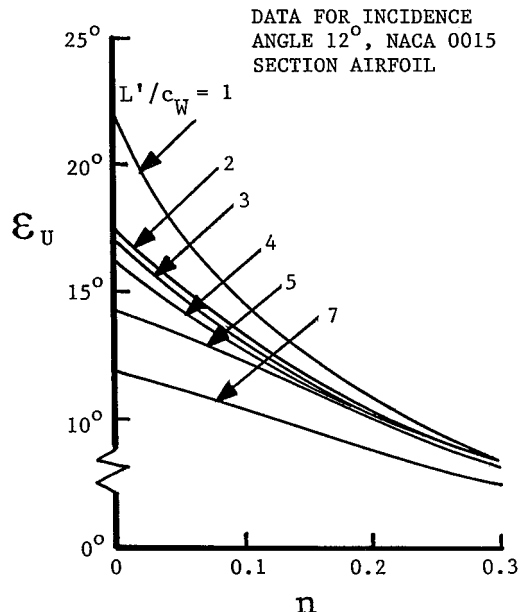


Fig. 3 Variation of upwash flow with downwind displacement  $L'/c_W$ .

wing. Each solid line represents results obtained in the University of Calgary facilities, with the OHS stabilizer surfaces removed, for aspect ratios covering the range  $4 \leq A_W \leq 11$ . There is no apparent influence of aspect ratio. The dotted lines were derived from the data of McAlister and Takahashi<sup>10</sup> for a Reynolds number of  $1.5 \times 10^6$ . Although the McAlister and Takahashi data extend only to be an  $n$  value of 0.3, it can be seen that there is reasonable agreement between the solid and dotted curves tending to confirm that near-wing-tip flows are not strong functions of wing-chord-based Reynolds number.

The results of McAlister and Takahashi<sup>10</sup> can also be used to establish the variation of upwash flow angle  $\epsilon_U$  with tail surfaces absent, as a function of the tail downwind displacement parameter  $L'/c_W$ . These results are presented, for an angle of incidence of 12 deg for McAlister and Takahashi's NACA 0015 aspect ratio 6.6 wing section at a Reynolds number of  $1.5 \times 10^6$  in Fig. 3. The range of  $L'/c_W$  values of practical interest for the present study is from 2 to 4. Within that range it appears that to a first order of approximation the upwash flow angle, as a function of  $n$ , is independent of  $L'/c_W$ .

### Horizontal Stabilizer Upwash Flowfield

Tests similar to those reported in the preceding section with no tail surfaces attached to the tail support boom were carried out, with the vertical stabilizer installed at the location of the horizontal stabilizer

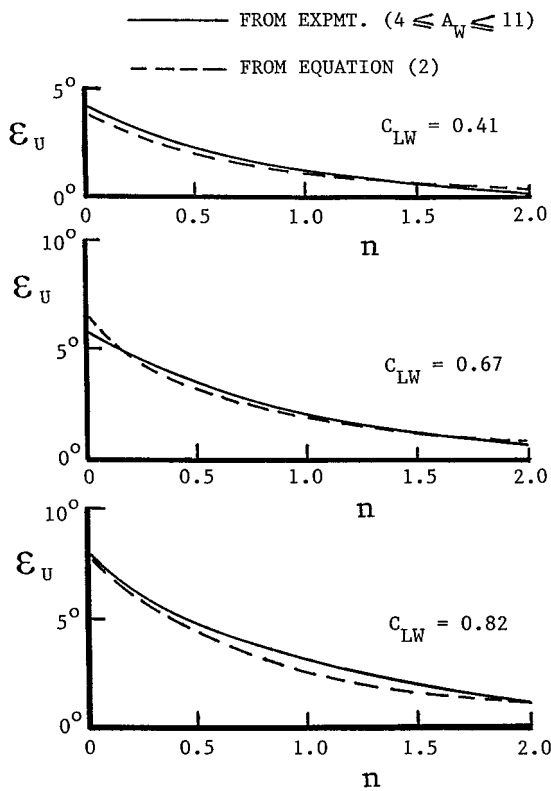


Fig. 4 Upwash flow angle over horizontal stabilizer.

that was omitted for these tests. Variable aspect ratio, over the range  $4 \leq A_W \leq 11$ , was simulated by projecting an available NACA 0018 section airfoil of uniform chord through a splitter plate installed in the wind tunnel to represent a plane of symmetry between the portion of the OHS configuration modeled and that which was omitted. The wing tip projecting into the test area was provided with a tail-support boom and also, as stated earlier, a vertical stabilizer surface.

The results obtained in this manner are represented by the solid lines of Fig. 4. The dotted curves illustrate the output of an analytical equation modeling the potential flow of a wing-tip vortex far downstream of an aircraft, specifically,

$$\frac{w}{U} = \frac{C_{LW}}{A_W} \frac{4}{\pi^2} \left\{ \frac{1}{1 - [(4/\pi)Y]^2} \right\} \quad (1)$$

modified empirically to describe the angle  $\epsilon_U$  of the upwash flow in the region  $2 \leq L'/c_W \leq 4$ , with account taken of the observed independence of  $\epsilon_U$  on  $A_W$ , the replacement of  $Y$  in terms of  $n$ , and the outward displacement from the wing tip of the horizontal stabilizer by the thickness of the boom, namely  $0.1 c_W$ . These modifications led to the final result when  $\epsilon_U$  is expressed in degrees:

$$\epsilon_U = C_{LW} \left\{ \frac{3.871}{[(4/\pi)(1.0333 - n/3)]^2 - 1} \right\} \left( 1.7667 - \frac{n}{3} \right) \quad (2)$$

#### Vertical Stabilizer Lateral Flowfield

Wind-tunnel tests were also carried out to establish the lateral, or inwash, flowfields acting on the vertical stabilizers. For this work the vertical stabilizer surface of the half-model OHS configuration was removed, and the horizontal stabilizer surface was installed at a realistic decalage angle of  $-6$  deg relative to the wing.

Similar to the upwash flow situation, it was found that the inwash flow was effectively independent of the main-plane aspect ratio  $A_W$ . The results obtained are presented as solid lines in Fig. 5. The dotted curves represent the results obtained from use of Eq. (2) multiplied by a factor of 1.6, thus,

$$\epsilon_L = 1.6\epsilon_U \quad (3)$$

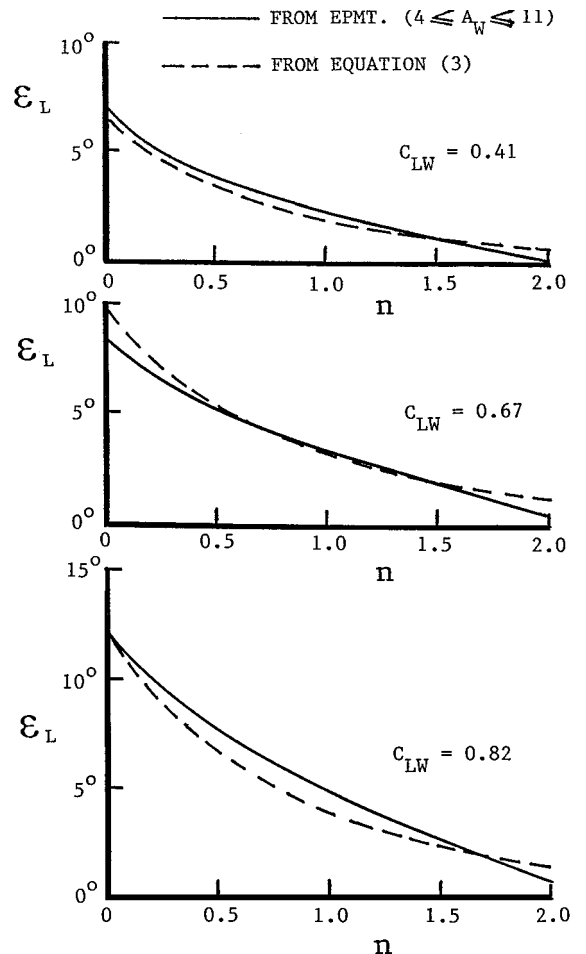


Fig. 5 Inwash, or lateral, flow angle over vertical stabilizer.

where  $\epsilon_U$  was evaluated from Eq. (2). It is clear that the fit to the experimental results is not quite as good as for the upwash case, although it appears to be adequate for preliminary design purposes.

#### Pitch Stability

In a previous study of a relatively conservatively designed OHS vehicle and a comparable conventional aircraft, each of aspect ratio six, the influences of three values of the static pitch margin  $\theta$  of 0.17, 0.23, and 0.32 were compared.<sup>1</sup> For the present study it was decided to maintain a constant  $\theta$  value of 0.23 for all cases. However, because  $\theta$  is defined as the distance from the neutral point to the c.g. divided by the wing chord, an increase in aspect ratio implies, for aircraft of prescribed wing area, a reduction of absolute static stability in pitch.

In a previous study of OHS and conventional aircraft of aspect ratio six,<sup>1</sup> the Oswald efficiency factor of the main-plane was assigned the conservative value of 0.8. Here the values of Oswald efficiency were evaluated from an empirical relationship, attributed to Cavallo,<sup>11</sup> applicable to straight wings in the form

$$e = 1.78(1 - 0.045A^{0.68}) - 0.64 \quad (4)$$

Equation (4) purports to be based on data derived from real aircraft and to include the adverse influence, on wing performance, of the junction between the main-plane and the fuselage. Equation (4) was also applied to the horizontal stabilizers of the conventional aircraft studied. Because the interaction of flaps on aircraft performance and the elevator settings required to maintain level flight over a range of wing lift coefficients have been investigated in detail in a previous study,<sup>1</sup> as have roll and directional control,<sup>5</sup> these topics are not considered here. In the present study attention is confined to establishing the comparative influences of main-plane aspect ratio on the performances of OHS configurations and otherwise comparable

conventional aircraft over a range of lift coefficients, in straight, level flight.

### Configurations Investigated

The configurations investigated in the study include only the aerodynamic surfaces (no fuselages or tail booms) of OHS and otherwise comparable conventional configurations. For all of the turbulent flow studies, the wing section selected was NACA 2412, and that for the horizontal and vertical stabilizers was NACA 0012. For all of the OHS configurations, the c.g. location was assumed to be 65% of the wing chord aft of the wing leading edge and for the conventional configurations 25% aft of the wing leading edge. It was also assumed, for all turbulent flow studies, that for all aerodynamic surfaces the two-dimensional drag coefficient  $C_{DO}$  had a value of 0.008 to allow for the presence of hinge lines where movable control surfaces joined the fixed portions of the aerodynamic surfaces. For simulated laminar-flow operation,  $C_{DO}$  was relaxed to a value of 0.005, where it is assumed that good sealing and fairing was provided between the fixed and movable portions of the aerodynamic surfaces of the laminar-flow wing and tails.

The horizontal-taillift coefficient  $C_{LTH}$  necessary to sustain level flight was evaluated by moments leading to the result

$$C_{LTH} = \frac{(a/c_w)C_{LW} + C_{M(c/4)W} + (c_{TH}S_{TH}/c_wS_w)C_{M(c/4)TH}}{(S_{TH}/S_w)(L'/c_w - a/c_w)} \quad (5)$$

where  $C_{M(c/4)TH}$  is zero for the cases considered here for zero elevator trim because symmetric sections were selected for the horizontal stabilizers of both the OHS and conventional aircraft. When  $C_{LTH}$  derived from Eq. (5) was not compatible with prevailing conditions, the elevators were assumed to be positioned to adjust  $C_{LTH}$  to the required value deduced from Eq. (5).

For the effective upwash and inflow angles impinging on the tails of OHS configurations, area-weighted analyses were performed on the half-tapered tail surfaces incorporating values of  $\varepsilon_U$  and  $\varepsilon_L$  obtained from Eqs. (2) and (3), respectively, yielding  $\bar{\varepsilon}_U$  and  $\bar{\varepsilon}_L$  in terms of  $C_{LW}$  for prescribed tail-surface aspect ratios. The latter were based, for reasons given earlier,<sup>1</sup> on twice the span of each tail half-surface. The downwash, due to the wings, at the tails of conventional aircraft was established using a procedure described by McCormick.<sup>12</sup>

On the basis of guidance derived from Figs. 4 and 5, it can be seen that influence of the wing-tip flow prevails for a maximum spanwise direction, and also vertically, for a distance approximately equal to twice the chord of the wing. It was found subsequently for OHS configurations that the best performances were obtained when each horizontal stabilizer projected two wing chords outboard of the tail-support boom. However, it was also found that the best vertical stabilizer performances were obtained with slightly shorter, and therefore lower aspect ratio, vertical stabilizers thereby giving a better trade-off between induced drag and  $\bar{\varepsilon}_L$ . The substantially optimized OHS configurations obtained in this manner for  $A_w$  values of 6, 9, 12, and 15 are presented in Fig. 6 for a static margin of 0.23. The relevant geometric details are shown in Fig. 7. The corresponding conventional configurations are presented in Fig. 8. For all of the conventional

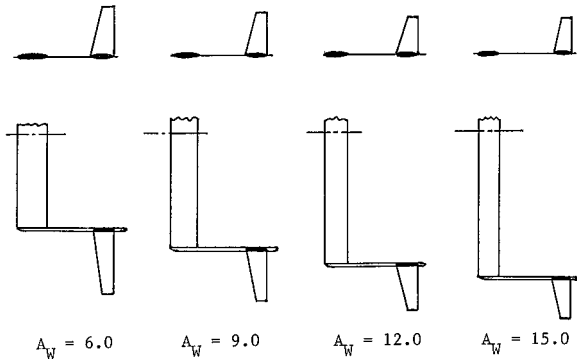


Fig. 6 Optimized OHS configurations studied ( $\theta = 0.23$ ).

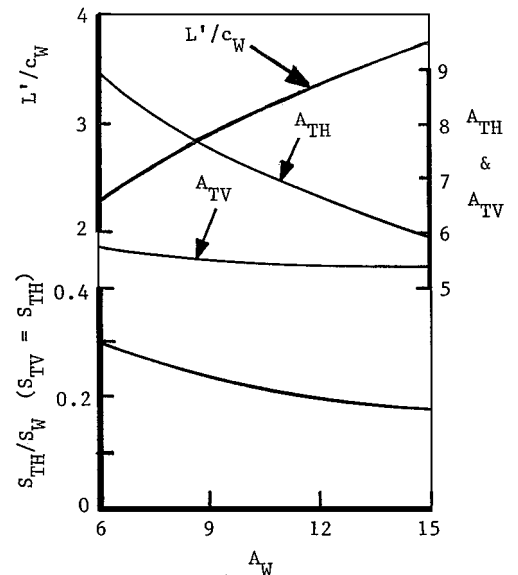


Fig. 7 Geometric parameters of the optimized OHS configurations.

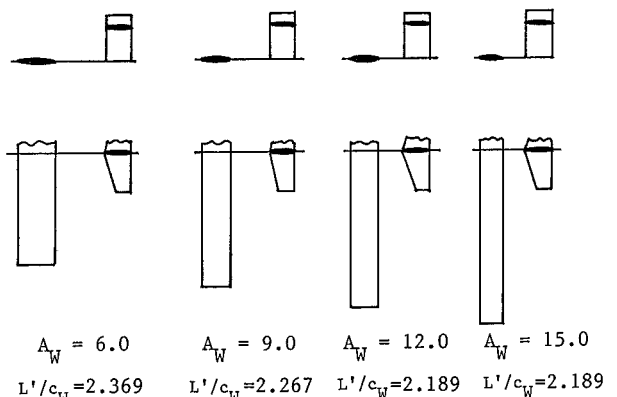


Fig. 8 Comparative conventional configurations ( $\theta = 0.23$ ).

arrangements, the horizontal stabilizer area divided by the wing area  $S_{TH}/S_w$  was 0.2 with a horizontal stabilizer aspect ratio  $A_{TH}$  of 4. The vertical stabilizer area was 75% of that of the horizontal stabilizer. For the OHS designs the area of the vertical stabilizers was made equal to that of the corresponding horizontal tails.

### Predicted Performances

Figure 9 shows the predicted performance lift/drag ( $L/D$ ) vs  $C_{LW}$ , for the OHS-type arrangements of aerodynamic surfaces. The locus of the peaks shows that the highest  $C_{LW}$  values range from approximately 0.64 with  $A_w = 6$  to nearly 0.71 when  $A_w = 15$ . The applicable wing-chord-based Reynolds number is  $6 \times 10^6$ .

Corresponding data for the comparable conventional configurations is presented in Fig. 10 for the same  $C_{LW}$  range. Here the peak values of  $C_{LW}$  range from 0.45 when  $A_w = 6$  to nearly 0.6 when  $A_w = 15$ . Figure 11 shows a comparison of the OHS and conventional data for equal lifts in terms of the ratio of OHS drag divided by that of corresponding conventional configurations vs  $C_{LW}$  with parameters of  $A_w$ . It can be seen from Fig. 11 that the relative advantage of the OHS arrangement tends to diminish as  $A_w$  is increased and to increase as  $C_{LW}$  increases. Figure 12 presents another form of performance comparison based on the loci of the peaks in Figs. 9 and 10. Here it can be seen that the  $L/D$  ratio of the conventional is, essentially, 69% of that of the OHS configuration of equal  $A_w$  over the range  $6 \leq A_w \leq 15$ .

It seems likely that very high aspect ratio configurations would incorporate laminar-flow surfaces. Accordingly, Fig. 13 offers a performance comparison, for an  $A_w$  value of 15, between OHS and conventionally configured arrangements. The airfoils selected were

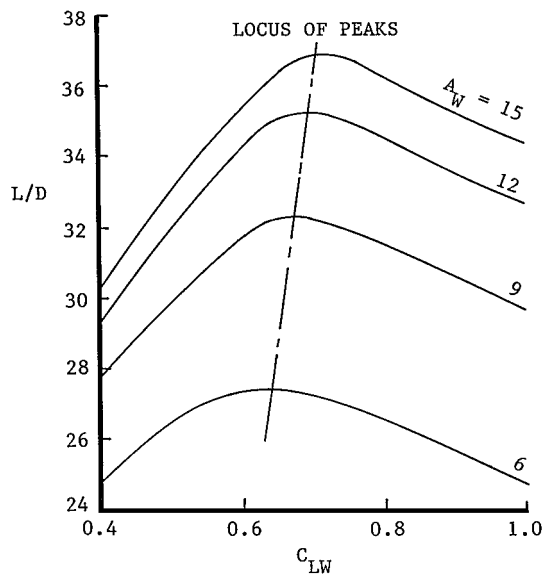


Fig. 9  $L/D$  of aerodynamic surfaces vs  $C_{LW}$  of optimized OHS configurations.

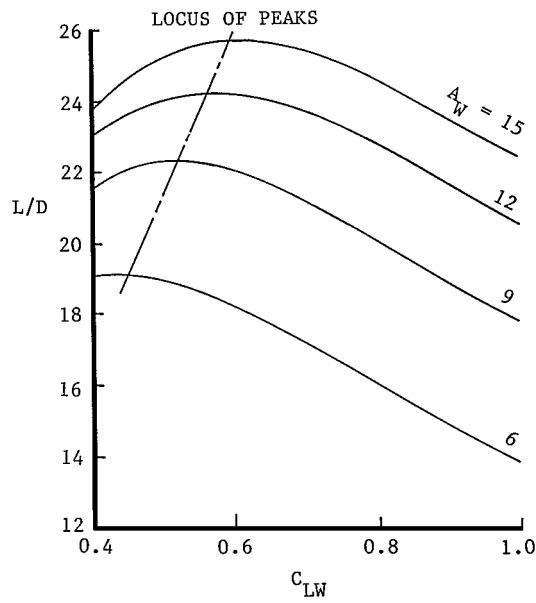


Fig. 10  $L/D$  of aerodynamic surfaces vs  $C_{LW}$  of comparative conventional configurations.

NACA 65<sub>2</sub>-415 for wings and NACA 64<sub>2</sub>-015 for tail surfaces. The  $C_{LW}$  range covered is reduced relative to the turbulent flow comparisons of Figs. 9-12 due to the need to remain within the drag bucket regions of the airfoils. The optimum  $C_{LW}$  value for the conventional configuration is approximately 0.47 whereas it is 0.58 for the OHS configuration. Comparison of Fig. 13 with Fig. 11 shows that the decay of the ratio of the OHS drag to that of the conventional configuration is more rapid for the laminar case than that applicable to turbulent flow.

### Discussion

An important finding from the wind-tunnel experiments was that  $\varepsilon_U$  and  $\varepsilon_L$  distributions were essentially independent of  $A_W$  although proportional to  $C_{LW}$ . The results due to McAlister and Takahashi,<sup>10</sup> although over a smaller range of aspect ratio and  $n$  than the University of Calgary work, tended to confirm the conclusion relating to the lack of dependence on  $A_W$ .

Because of the attempt to optimize the OHS configurations to maximize aerodynamic performance, within the limitations of the analytical processes employed, the results presented in Figs. 11-13

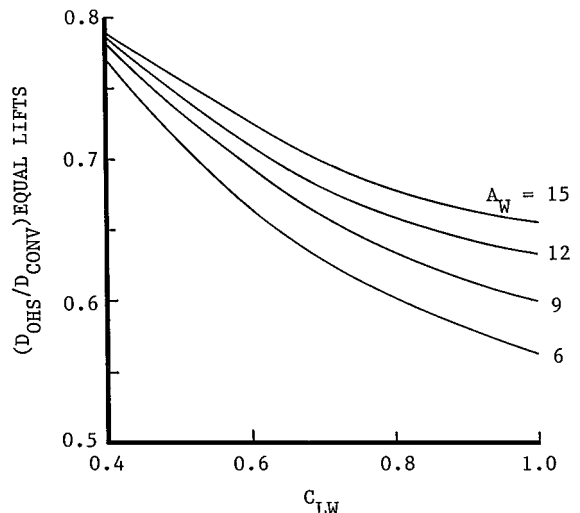


Fig. 11 Ratio of drags of OHS aerodynamic surfaces to those of conventional configurations vs  $C_{LW}$  for turbulent flow conditions.

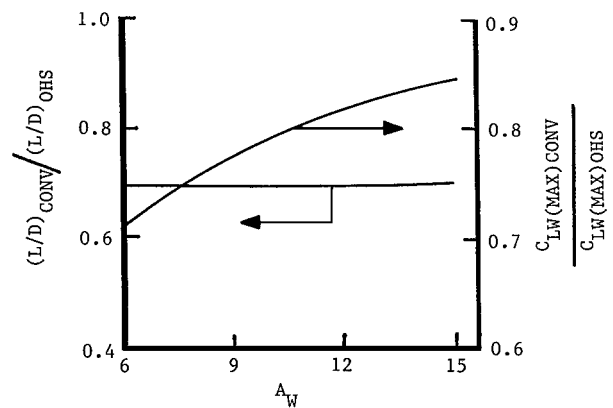


Fig. 12 Comparison of  $L/D$  ratios and  $C_{LW}$  ratios based on loci of peaks presented in Figs. 9 and 10.

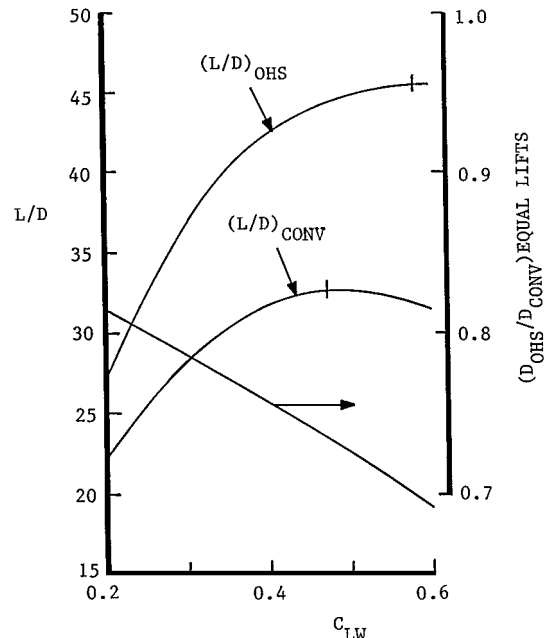


Fig. 13 Ratio of drag of OHS aerodynamic surfaces to that of a corresponding conventional configuration, laminar-flow conditions ( $A_W = 15$ ).

appear to represent the relative performances of OHS configurations, for both turbulent and laminar flows, in the most favorable light. A general observation was that the relative advantage of OHS configurations over conventional designs diminishes as aspect ratio  $A_w$  increases. However, extrapolation of the data generated in the present study suggests that substantial relative advantages prevail for OHS configurations with  $A_w$  values much greater than 15.

Generally, the results obtained from the present study are in line with, although better than, those from earlier wind-tunnel tests carried out for wing aspect ratios of approximately six (Ref. 3). The primary reason for this appears to be the optimized OHS configuration applicable to this study whereas the tail surfaces of the wind-tunnel model were of low aspect ratio and were not optimized. A previous analytical study for a wing aspect ratio of six featuring low aspect ratio tail surfaces produced a result substantially in agreement with the experimental wind-tunnel findings.<sup>1</sup>

An important deduction from the study was that for a common value of  $C_{LW}$ , an OHS configuration is typically about 15% smaller in wing planform area than a conventional aircraft of equal lift. However, when the comparison is based on maximum  $L/D$  values, the OHS configuration is an additional 30% smaller in planform area and correspondingly lower in drag. This implies, however, the need for a 14% greater takeoff speed or, possibly, the use of more sophisticated flaps, etc. Alternately, if the 30% reduction in planform area is not implemented, an OHS aircraft can cruise at a greater altitude, with better economy, than an otherwise comparable conventional design.

Essentially second-order factors not accounted for in the present study include, for conventional configurations, the influence on the wing of the circulation around the horizontal stabilizer, a subject discussed in detail by Laitone.<sup>13</sup> For a negatively lifting tail, this effect would be expected to worsen, very slightly, the wing performance. For OHS configurations the lifting tails would be expected, from similar reasoning, to augment favorably, by a very small margin, the wing upwash flow. A concern with OHS aircraft is the extent of the immersion of the tail surfaces in what, for all practical purposes, is the finite flowfield generated by wing-tip spillage. A simple analysis, not presented here, suggests that this consideration does not represent a serious problem; nevertheless, it is one that should be taken into account. It appears that premature stalling of OHS tail surfaces tends to be inhibited due to a washout effect, even with nontwisted tail surfaces, due to the reduction of  $\epsilon_U$  and  $\epsilon_L$  with increasing distance from the tail boom (Figs. 4 and 5).

A preliminary, restrictive, structural loading study<sup>3</sup> showed that, for an OHS configuration with  $A_w = 6$  employing a wing of symmetric section, the wing torsional loadings and wing-root bending moments, for such a configuration in steady flight, are approximately equal to those of a comparable conventional aircraft. However, more work is required to investigate the loading of OHS configurations more generally to ensure that increased structural loads relative to conventional aircraft, and hence greater structural weight, are not major problems. To date, for one specific case, a flutter analysis has been undertaken, by Scaled Composites, for the full-scale environmental monitoring UAV referred to earlier. It was found, for that particular aircraft, that flutter was not a concern anywhere within the mission envelope. Again, more work is required to come to more general conclusions relating to the potential for OHS configuration to suffer from, or avoid, aeroelastic difficulties.

## Conclusions

The following conclusions are drawn from the study:

- 1) Upwash flow and inflow at the tails of OHS configurations are essentially independent of main-plane aspect ratio  $A_w$  but proportional to the main-plane lift coefficient  $C_{LW}$ .
- 2) On an  $L/D$  basis, OHS configurations are substantially better than those of conventional type of equal aspect ratio  $A_w$ . However, the OHS relative advantage tends to diminish as  $A_w$  increases. With OHS and conventional designs of equal  $A_w$ , the OHS design exhibits relatively greater  $L/D$  values when both are provided with laminar-flow aerodynamic surfaces.
- 3) For equal  $A_w$ ,  $C_{LW}$ , and gross lift, an OHS configuration is, typically, about 15% smaller in wing planform area than a conventional aircraft.
- 4) The maximum  $L/D$  values for OHS aircraft occur, typically, at  $C_{LW}$  values that are from 16 to 30% greater than for conventional designs of equal main-plane aspect ratio  $A_w$ .

## Acknowledgments

The writer is grateful to numerous students of the Department of Mechanical and Manufacturing Engineering of the University of Calgary who have, over a period of years, contributed to the development of outboard-horizontal-stabilizer (OHS) systems by building radio-controlled OHS model aircraft. Thanks are also due to Roland Siemonsen of Kingston, Ontario, and Peter Thannhauser of Calgary, Canada, both of whom have served as very capable pilots of these models.

## References

- <sup>1</sup>Kentfield, J. A. C., "Upwash Flowfields at the Tails of Aircraft with Outboard Horizontal Stabilizers," AIAA Paper 98-0757, Jan. 1998.
- <sup>2</sup>Kentfield, J. A. C., "Aircraft Configurations with Outboard Horizontal Stabilizers," Rept. 440, Dept. of Mechanical Engineering, Univ. of Calgary, Calgary, Alberta, Canada, Jan. 1990.
- <sup>3</sup>Kentfield, J. A. C., "Case for Aircraft with Outboard Horizontal Stabilizers," *Journal of Aircraft*, Vol. 32, No. 2, 1995, pp. 398-403.
- <sup>4</sup>Kentfield, J. A. C., "Aircraft Configurations with Outboard Horizontal Stabilizers," *Journal of Aircraft*, Vol. 28, No. 10, 1991, pp. 670-672.
- <sup>5</sup>Kentfield, J. A. C., "The Flight Characteristics of a Commuter Aircraft Employing Outboard Horizontal Stabilizers," SAE Paper 965610, Oct. 1996.
- <sup>6</sup>Kentfield, J. A. C., "The Aspect-Ratio Equivalence of Conventional Aircraft with Configurations Featuring Outboard Horizontal Stabilizers," *Transactions of the SAE, Journal of Aerospace, Section 1*, Vol. 106, 1997, pp. 1733-1741; also Paper 975591.
- <sup>7</sup>Schoeni, A., "The Flying Pancakes," *Aeroplane Monthly*, Vol. 3, No. 12, 1975, pp. 624-627.
- <sup>8</sup>Combat Aircraft 1945-1960, Sampson Low, Maidenhead, Berkshire, England, U.K., 1980, p. 20.
- <sup>9</sup>Tipton, B. J., Smith, D. E., and Mullins, B. R., "The Aerodynamics and Performance Analysis of a Unique Semi-Tailless Aircraft," AIAA Paper 96-0408, Jan. 1996.
- <sup>10</sup>McAlister, K. W., and Takahashi, R. K., "NACA 0015 Wing Pressure and Trailing Vortex Measurements," NASA TP-3151, 1991; also U.S. Army Aviation Systems Command, TR 91-A-003, 1991.
- <sup>11</sup>Cavallo, B., "Subsonic Drag Estimation Methods," U.S. Naval Air Development Center Rept. NADC-AW-6604, 1966.
- <sup>12</sup>McCormick, B. W., *Aerodynamics, Aeronautics and Flight Mechanics*, 2nd ed., Wiley, New York, 1995, Chap. 12, pp. 473-482.
- <sup>13</sup>Laitone, E. V., "Positive Tail Loads for Minimum Induced Drag of Subsonic Aircraft," *Journal of Aircraft*, Vol. 15, No. 12, 1978, pp. 837-842.